THE JOURNAL OF PHYSICAL CHEMISTRY B LETTERS

2006, *110,* 2968−2971
Published on Web 02/01/2006

Soft-Landing Isolation of Vanadium−Benzene Sandwich Clusters on a Room-Temperature Substrate Using *n*-Alkanethiolate Self-Assembled Monolayer Matrixes

Masaaki Mitsui,[†] Shuhei Nagaoka,[†] Takeshi Matsumoto,[†] and Atsushi Nakajima*[,†,‡]

Department of Chemistry, Faculty of Science and Technology, Keio University, 3-14-1 Hiyoshi, Kohoku-ku, Yokohama 223-8522, Japan, and CREST, Japan Science and Technology Agency (JST), c/o Department of Chemistry, Keio University, Yokohama 223-8522, Japan

Received: December 9, 2005; In Final Form: January 6, 2006

Gas-phase synthesized vanadium−benzene 1:2 (VBz_2) sandwich clusters were size-selectively deposited onto bare gold and long-chain *n*-alkanethiolate [$-S-(CH_2)_{n-1}-CH_3$; $n = 16$, 18, and 22] self-assembled monolayer (SAM)-coated gold substrates under ultrahigh vacuum (UHV) conditions. Investigation of the resulting deposited clusters was performed by infrared reflection absorption spectroscopy (IRAS) and thermal desorption spectroscopy (TDS). The IR frequencies of the soft-landed VBz_2 clusters show excellent agreement with the fundamentals reported in IR data of VBz_2 in an argon matrix. The analysis of IRAS spectra reveals that while there was no orientational preference of the VBz_2 clusters on a bare gold substrate, the VBz_2 clusters deposited onto the SAM substrates were highly oriented with the molecular axis 70−80° tilted off the surface normal. In addition, analysis of TDS spectra revealed unusually large adsorption heats of the physisorbed VBz_2 clusters. The present results are explained by cluster penetration into the long-chain alkanethiolate SAM and for the first time demonstrate the matrix isolation of gas-phase organometallic clusters around room temperature.

One-dimensional (1D) transition metal−benzene organometallic compounds are generating increasing interest due to their unique size-dependent characteristics and potential applications in nanodevices. In this class of compounds, vanadium−benzene clusters (V_nBz_{n+1}) have been spotlighted especially because of the efficient formation of 1D multiple-decked sandwich structures,[1−5] their quasi-band electronic structure,[6] and their ferromagnetic properties.[7,8]

Nondestructive deposition of mass-selected cluster ions onto suitable substrates, so-called "soft-landing", can offer a promising route to design and fabricate cluster-based materials with desirable properties. In the pursuit of this ambitious goal, it is important to establish a technique of controlling the thermal stability and adsorption structure of the resulting soft-landed clusters. So far, soft-landing into an inert rare gas substrate has been successfully applied to metal[9] and organometallic clusters.[10] In this technique, the rare gas serves as a buffer layer to keep the clusters intact upon deposition onto a substrate. However, the rare gas layer evaporates even at a very low temperature, leaving the clusters on the substrate surface. As a result, the nature of the cluster−surface interaction dominates the adsorption structure, energetics, and thermal stability of the soft-landed clusters. When the resulting clusters are weakly physisorbed on the substrate, their structures are relatively unperturbed and retain many of the properties of their gas-phase counterparts. This is a key requirement for the organometallic sandwich clusters, because their unique properties originate from their 1D sandwich structures.[6−8] However, such a weak surface interaction usually permits thermal desorption of the clusters well below room temperature because of a relatively small desorption activation energy (or adsorption heat) of physisorption.[11−13] Hence, it is highly desirable to achieve a much larger adsorption heat of the soft-landed clusters while keeping them intact on the substrate.

Herein, we report a method to allow us to realize a room-temperature isolation of gas-phase synthesized organometallic sandwich clusters on solid substrates while maintaining their native structures. The vanadium−benzene 1:2 (VBz_2) clusters produced in the gas phase were size-selectively soft-landed onto bare gold and long-chain *n*-alkanethiolate self-assembled monolayer (SAM)-coated gold substrates. The resulting adsorbed clusters were investigated by the infrared reflection absorption spectroscopy (IRAS) and thermal desorption spectroscopy (TDS) experiments to determine the orientation and adsorption heat of the adsorbed VBz_2 clusters. On the basis of the results, we will discuss why the VBz_2 clusters deposited onto the SAM substrate exhibit clear orientational preference as well as high thermal stability.

The soft-landing apparatus has been described elsewhere.[10,14,15] Briefly, it consists of a cluster source, a mass selection stage, and a deposition chamber where the IRAS and TDS measurements are conducted. VBz_2 cations were produced in the expansion from a piezo-driven pulsed valve under a He stagnation pressure of 4 atm by the reaction between laser-vaporized vanadium and benzene vapors. The cations thus produced were guided by a series of ion optics, separated from the neutrals and anions by a quadrupole deflector, and size-

* To whom correspondence should be addressed. E-mail: nakajima@chem.keio.ac.jp.
[†] Department of Chemistry, Faculty of Science and Technology, Keio University.
[‡] CREST, Japan Science and Technology Agency (JST), c/o Department of Chemistry, Keio University.

10.1021/jp057194v CCC: $33.50

selected by a quadrupole spectrometer; subsequently, the clusters were deposited onto a substrate with a collision energy of 20 ± 10 eV under ultrahigh vacuum (UHV) conditions (~10^{-10} Torr). The substrate was cooled to 200 K, and the total amount of the deposited cluster ions was determined by monitoring the ion current on the substrate during the deposition time.

In the IRAS measurements, a Fourier transform infrared (FT-IR) spectrometer (Bruker IFS66v/S) operating at ~0.1 Torr was used. A collimated IR beam emerging through one of the side ports of the spectrometer was focused onto the sample substrate at an angle of incidence of ~80° with respect to the surface normal through a flat KBr window. After reflection from the sample, the IR beam exits the vacuum chamber through another KBr window and is directed onto an off-axis parabolic mirror, which refocuses the beam onto the active element of a liquid-nitrogen-cooled mercury cadmium telluride (MCT) detector. The detector and the lens system are mounted into a separate vacuum chamber pumped to a pressure of about 0.1 Torr to remove spectral background contributions due to atmospheric gases. All spectra were recorded with a spectral resolution of 2 cm^{-1}. Five hundred scans were accumulated for background and sample spectra, which were recorded before and after the cluster deposition, respectively. In the TDS experiments, which have been described elsewhere,[14,15] the substrate is positioned with the surface normal parallel to the quadrupole axis of the mass spectrometer and heated at 1 K/s. The desorbed species were detected by a mass spectrometer (4−4000 amu, 150-QC, Extrel). The reproducibility of the experimental data was confirmed at least three times in both the IRAS and TDS measurements.

In this study, a commercially available 10 × 10 mm^2 gold substrate, Au/Ti/silica (Auro Sheet, Tanaka Precious Metal Co. Ltd.), was used. To remove organic contaminants from the surface, the substrate was immersed in a piranha solution. Solution-phase chemisorption was then conducted by immersing the chemically polished gold substrate in a 2 mM ethanolic solution of 1-hexadecanethiol (C_{16}, Wako), 1-octadecnethiol (C_{18}, Aldrich), and 1-docosylthiol (C_{22}, Narchem) for 1 day. The formation of SAM on the gold surface was confirmed by IRAS and contact angle measurements.[15]

Figure 1 shows the 650−1550 cm^{-1} region of typical IRAS spectra for VBz_2 clusters soft-landed on (a) bare gold and (b) C_{22}-SAM-coated gold substrates at 200 K. Their vibrational assignments based on previous studies[10,16−18] are provided in Table 1. In the present measurements, the *apparent* total amounts of the deposited clusters were set to provide a monolayer coverage (2 × 10^{14} clusters/cm^2). Comparison of the spectral feature intensities (e.g., signal-to-noise ratio) of the deposited clusters on the bare gold and C_{22}-SAM substrates shows that the soft-landing efficiency of the VBz_2 cluster cations with a high incident energy of ~20 eV is about 10 times higher for the C_{22}-SAM than for the bare gold substrate. This result indicates that, like the rare gas matrix, the SAM serves as an efficient buffer layer to reduce the collision-induced dissociation in the landing process. In the case of the bare gold substrate, therefore, the actual coverage of the deposited clusters may be much less than 1.0.

In all of the spectra, four IR absorption peaks are observed at 747, 956, 988, and 1418 cm^{-1} within ±1 cm^{-1} and compare well to the fundamentals reported in IR data of VBz_2 in an Ar matrix,[16] which is also shown as a top trace in Figure 1. The close similarity of the IR absorption frequencies to those observed in the Ar matrix indicates that the soft-landed VBz_2 cluster cations lose their charge and the resulting neutral clusters physisorb on both the bare gold and C_{22}-SAM substrates, while

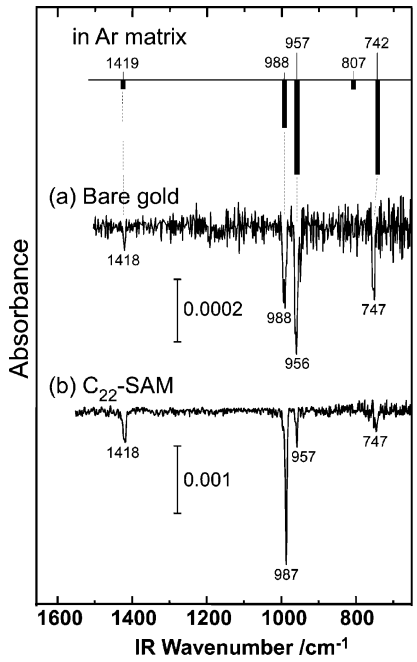

Figure 1. Representative IRAS spectra of the adsorbed VBz_2 clusters on (a) bare gold and (b) C_{22}-SAM-coated gold substrates taken after 2 × 10^{14} VBz_2 cation deposition onto each substrate at 200 K. A bar plot of the reported IR fundamentals for VBz_2 in the Ar matrix[16] is also shown as the top trace.

TABLE 1: Measured Fundamentals of the IRAS Spectra of Adsorbed VBz_2 Clusters and Their Assignments

		support				
mode[a]	symmetry	Ar matrix[b]	bare gold	C_{16} SAM	C_{18} SAM	C_{22} SAM
$\upsilon_{o\text{-}p}$(CH)	A_{2u}	742	747	747	747	747
υ_t(CC)	A_{2u}	957	956	956	956	957
$\upsilon_{i\text{-}p}$(CH)	E_{1u}	988	988	988	988	987
υ(CC)	E_{1u}	1419	1418	1418	1418	1418

[a] Vibrational modes: $\upsilon_{o\text{-}p}$(CH), CH out-of-plane bending; υ_t(CC), ring breathing; $\upsilon_{i\text{-}p}$(CH), CH in-plane bending; υ(CC), in-plane CC ring stretching and deforming. [b] Reference 16.

maintaining their native sandwich structures. However, the relative intensities of the four bands are strikingly different between the VBz_2/C_{22}-SAM and VBz_2/Au (or Ar matrix) spectra. It is important to note that similar results are also obtained for the C_{16}-SAM and C_{18}-SAM substrates.

Assuming an idealized D_{6h} structure of the adsorbed VBz_2 cluster, vibrational modes with A_{2u} and E_{1u} symmetry are IR active and can potentially give rise to intense IR absorption peaks, depending on the cluster orientation with respect to the substrate surface. Indeed, the two A_{2u} modes at 747 and 956 cm^{-1} and the two E_{1u} modes at 988 and 1418 cm^{-1} are observed in the IRAS spectra for a VBz_2 cluster on the bare Au and C_{22}-SAM/gold substrates. As shown in Figure 2, vibrational modes with A_{2u} symmetry cause a transition dipole moment vector (μ) along the D_{6h} symmetry molecular axis of the VBz_2 cluster, while modes with E_{1u} symmetry cause dipole moments perpendicular to it. Using the surface IR selection rule, the relative intensities of the A_{2u} and E_{1u} modes qualitatively reflect the orientation of the adsorbed VBz_2 clusters. Thus, the four bands, two A_{2u} (747 and 956 cm^{-1}) and two E_{1u} (988 and 1418 cm^{-1}), are useful in gaining insight into the adsorbed VBz_2 cluster orientation.

Since the VBz_2 clusters isolated in the Ar matrix are randomly oriented in space, the similarity of the relative intensities of the

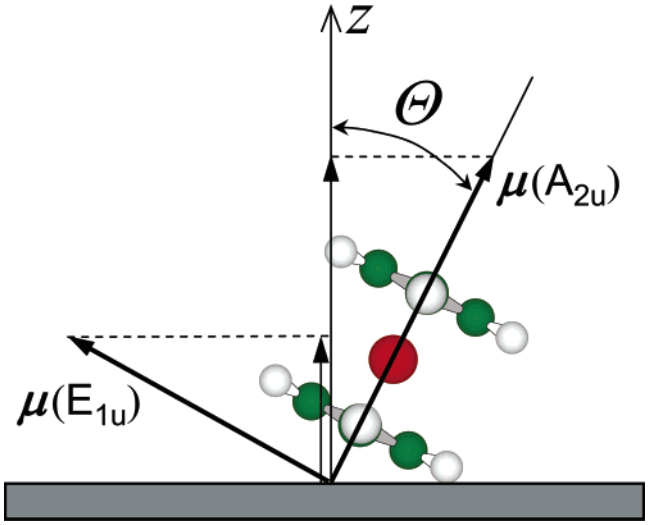

Figure 2. Orientation angle (Θ) of the transition dipole moments (μ) of vibrational modes with A_{2u} and E_{1u} symmetries of VBz_2 at the surface.

TABLE 2: Orientation Angle (Θ, deg), Adsorption Heat (E_d, kJ/mol), and Desorption Order (n) of Adsorbed VBz_2 Clusters

substrate	Θ	E_d	n
bare gold		64 ± 13	2
C_{16} SAM	73 ± 2	130 ± 10	1
C_{18} SAM	72 ± 1	138 ± 21	1
C_{22} SAM	78 ± 6	153 ± 27	1

A_{2u} and E_{1u} modes in the VBz_2/gold spectrum to those observed in the Ar matrix spectrum indicates random orientation of the adsorbed VBz_2 clusters on the gold substrate. Meanwhile, comparing the spectral intensities of the adsorbed VBz_2 clusters on the SAM substrate and the corresponding bands in the Ar matrix spectrum, it is evident that the two E_{1u} modes at 988 and 1418 cm^{-1} are relatively intense and the two A_{2u} modes at 747 and 957 cm^{-1} are very weak. Besides, the relative intensities of the observed A_{2u} and E_{1u} modes are nearly independent of the apparent cluster coverage (θ) in the range $\theta = 0-1.0$. This result qualitatively suggests that the molecular axis of the adsorbed VBz_2 clusters is substantially tilted toward the surface plane.

We have made a semiquantitative determination of the tilt angle (Θ) of an adsorbed cluster relative to the surface normal using the RATIO method proposed by Debe.[19,20] The absorption intensity [$I(G)$] for a mode with "G" symmetry having transition dipole moment vector $\mu(G)$ is given by $I(G) \propto NE_z^2\mu_z(G)^2$, where N is the number of adsorbates and E_z and $\mu_z(G)$ are the components of the electric field and the transition dipole moment along the surface normal, respectively. The dependence of our measured vibrational mode intensities on the cluster coverage (θ) and the electric field intensity (E_z) can be removed by choosing to deal with only the intensity ratio of the A_{2u} and E_{1u} modes, $I(A_{2u})/I(E_{1u}) = [\mu_z(A_{2u})/\mu_z(E_{1u})]^2$. Assuming that the variation in the molecular orientation of VBz_2 clusters on a SAM substrate can be neglected, one can determine the tilt angle (Θ) of the cluster on the SAM substrate using

$$\sin^2 \Theta = 2/\{2 + [I^{SAM}(A_{2u})/I^{SAM}(E_{1u})]/[I^{Ar}(A_{2u})/I^{Ar}(E_{1u})]\} \quad (1)$$

where I^{SAM} indicates the absorption intensity in the oriented state (i.e., SAM substrate) and I^{Ar} indicates the corresponding intensity in the random orientation (i.e., Ar matrix). The analytical results are summarized in Table 2.

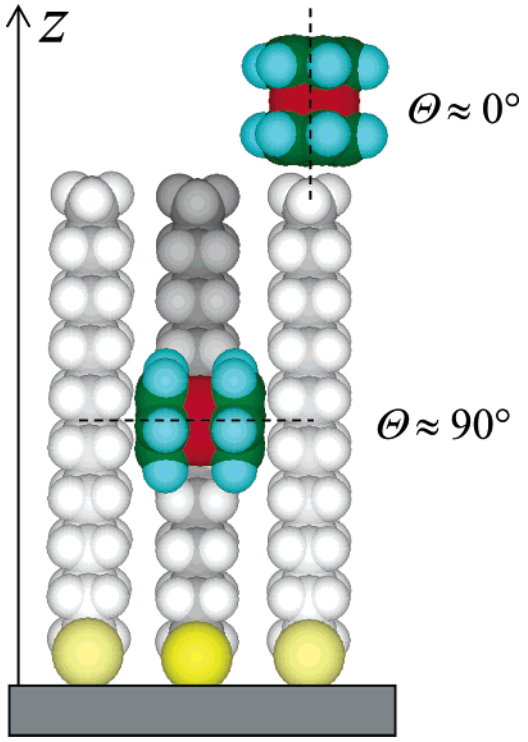

Figure 3. Schematic illustration of two proposed adsorption regimes, i.e., surface and internal trapping models, of VBz_2 on a long-chain alkanethiolate SAM substrate. The structural disorder in the alkanethiolates induced by the cluster adsorption are not shown here. In the case of adsorption on the outermost methyl group of the alkanethiolate, the molecular axis of the adsorbed cluster is nearly parallel with the surface normal (i.e., $\Theta \approx 0°$). In the internal trapping model, on the other hand, the molecular axis is canted $\Theta \approx 90°$ from the surface normal through the CH$-\pi$ interactions between the capping benzene rings of VBz_2 and the lateral methylene groups of alkanethiolates.

As shown in Figure 3, when the VBz_2 cluster is bound *on* a methyl end group of alkanethiolate, the cluster may favor the adsorption geometry with the relatively small tilt angle (i.e., $\Theta \approx 0$) because the highly tilted geometry should be accompanied by the repulsions between the hydrogen atoms of the VBz_2 cluster and the neighboring methyl groups. On the other hand, VBz_2 clusters incorporated in the SAM interact with the hydrogen atoms of the lateral methylene groups of the surrounding alkanethiolates. In this adsorption regime, the molecular axis of VBz_2 would be significantly canted from the surface normal as a result of the preferential CH$-\pi$ interaction between the capping benzene rings of VBz_2 and the lateral methylene groups, as also shown in Figure 3 ($\Theta \approx 90°$). Thus, the large tilt angles of the VBz_2 clusters, that is, $\Theta \approx 70-80°$, determined herein imply that the VBz_2 clusters are trapped *inside* the SAM.

To evaluate the thermal stability of the adsorbed VBz_2 clusters, the TDS spectra of the parent mass 207 (VBz_2) following deposition of 4×10^{13} VBz_2 cations ($\theta \approx 0.2$) onto bare gold and C_{22}-SAM/gold substrates at 200 K were recorded and are shown in Figure 4. The other common 51 (V), 78 (Bz), and 129 (VBz) mass fragments of VBz_2 yield TDS spectra identical to mass 207 and are not shown here. It is clear that the threshold desorption temperature on the C_{22}-SAM substrate (~300 K) is ~50 K higher than that on the bare gold substrate, suggesting that the clusters are rather strongly trapped on the SAM substrate relative to the gold substrate. It is important to note that the IR absorption peaks of the VBz_2 clusters soft-landed onto the long-chain SAM substrates were clearly observed up to a substrate temperature of ~300 K, while they

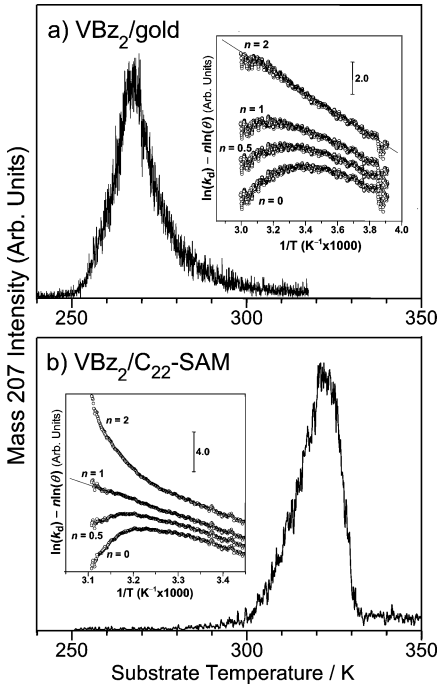

Figure 4. TDS spectra of VBz_2 parent mass 207 for the deposition of 4×10^{13} VBz_2 cations onto (a) bare gold and (b) C_{22}-SAM/gold substrates at 200 K. The insets show analysis of the TDS profile for the determination of adsorption heat (E_d) and desorption reaction order (n). The curves from bottom to top are for $n = 0$, 0.5, 1, and 2. For a bare gold substrate, the best linear fit is obtained with $n = 2$, whereas $n = 1$ for a C_{22}-SAM substrate. From the slope of the linear fit, the E_d values were determined and are listed in Table 2.

disappeared around 260 K in the case of the bare gold substrate.[15]

The TDS peak can be analyzed with the desorption order (n), prefactor (υ), and activation energy for desorption (i.e., adsorption heat, E_a) treated as variables in a $[\ln(k_d) - n \ln(\theta)]$ versus $[1/T]$ plot[21] with $k_d = d\theta/dT$. In the insets of Figure 4, we also show $[\ln(k_d) - n \ln(\theta)]$ versus $[1/T]$ plots, corresponding to TDS curves for desorption orders of $n = 0$, 0.5, 1, and 2. The plots were linear only for $n = 2$ for the bare gold and $n = 1$ for the SAM substrates. The slope of the linear fit yielded a value of 64 ± 13 kJ/mol for the adsorption heat of the clusters on bare gold. In the case of the C_{22} SAM, the adsorption heat was determined to be 153 ± 27 kJ/mol which is comparable to the typical adsorption heat of chemisorptions ($\sim$100 kJ/mol or $\sim$1 eV). Similar results, also listed in Table 2, were obtained for other long-chain SAM substrates.

The second-order desorption kinetics observed on the clean gold surface is likely due to the surface diffusion of the adsorbed clusters prior to desorption, because the diffusion activation energy on metal substrates is usually small enough to permit quasi-free two-dimensional diffusion of molecular adsorbates.[22] In addition, previous TDS studies have suggested that diffusion can induce a tailing on the higher temperature side of the peak, resulting in an apparent second-order desorption process.[11,12] On the other hand, the first-order desorption kinetics of VBz_2 on the long-chain SAM substrates indicates that the clusters are desorbed directly from the SAM without significant intercluster interactions. Moreover, the unusually large desorption activation energy (i.e., >1 eV) manifests the presence of a significant physical effect in the VBz_2 adsorption for the SAM substrate. By considering these results, it can be concluded that the VBz_2 clusters (whose size is $\sim$5 Å) penetrate into the long-chain C_{16-22} SAM (20−30 Å thickness[23]) and are physically trapped in the lateral void space between the alkanethiolate molecules. The penetration into the dense packing monolayer presumably prohibits two-dimensional diffusion of the clusters, leading to first-order desorption kinetics. In addition, a large activation energy would be needed in the desorption process because diffusion out from the SAM is likely accompanied by structural rearrangements of the neighboring alkanethiolates. This adsorption model is fully compatible with the above-mentioned IRAS results, where the orientation of the adsorbed VBz_2 clusters suggests the presence of a CH−π interaction between VBz_2 and the lateral methylene groups of alkanethiolates.

In summary, our results illustrate that VBz_2 sandwich clusters can be isolated near room temperature using a long-chain alkanethiolate SAM matrix. In addition, the SAM-matrix-isolated VBz_2 clusters are highly oriented due to their penetration into the SAM matrix. The room-temperature isolation technique established in this study is anticipated to open up new possibilities to enhance our understanding of organometallic sandwich cluster−support interactions and result in noticeable advantages for applications using such clusters.

Acknowledgment. This work is partly supported by the 21st Century COE program "KEIO LCC" from the Ministry of Education, Culture, Sports, Science, and Technology.

References and Notes

(1) Hoshino, K.; Kurikawa, T.; Takeda, H.; Nakajima, A.; Kaya, K. *J. Phys. Chem.* **1995**, *99*, 3053.
(2) Yasuike, T.; Nakajima, A.; Yabushita, S.; Kaya, K. *J. Phys. Chem. A* **1997**, *101*, 5360.
(3) Weis, P.; Kemper, P. R.; Bowers, M. T. *J. Phys. Chem. A* **1997**, *101*, 8207.
(4) Nakajima, A.; Kaya, K. *J. Phys. Chem. A* **2000**, *104*, 176.
(5) Yasuike, T.; Yabushita, S. *J. Phys. Chem. A* **1999**, *103*, 4533.
(6) Miyajima, K.; Muraoka, K.; Hashimoto, M.; Yasuike, T.; Yabushita, S.; Nakajima, A. *J. Phys. Chem. A* **2002**, *106*, 10777.
(7) Miyajima, K.; Nakajima, A.; Yabushita, S.; Knickelbein, M. B.; Kaya, K. *J. Am. Chem. Soc.* **2004**, *126*, 13203.
(8) Wang. J.; Acioli, P. H.; Jellinek, J. *J. Am. Chem. Soc.* **2005**, *127*, 2812.
(9) Harbich, W. *Philos. Mag. B* **1999**, *79*, 1307 and references therein.
(10) Judai, K.; Sera, K.; Amatsutsumi, S.; Yagi, K.; Yasuike, T.; Yabushita, S.; Nakajima, A.; Kaya, K. *Chem. Phys. Lett.* **2001**, *334*, 277.
(11) Vogt, A. D.; Beebe, T. P., Jr. *Langmuir* **1999**, *15*, 2755.
(12) Vogt, A. D.; Beebe, T. P., Jr. *J. Phys. Chem. B* **1999**, *103*, 8482.
(13) Lavrich, D. J.; Wetterer, S. M.; Bernasek, S. L.; Scoles, G. *J. Phys. Chem. B* **1998**, *102*, 3456.
(14) Nagaoka, S.; Okada, E.; Doi, S.; Mitsui, M.; Nakajima, A. *Eur. Phys. J. D* **2005**, *34*, 239.
(15) Nagaoka, S.; Matsumoto, T.; Okada, E.; Mitsui, M.; Nakajima, A. Manuscript to be published.
(16) Andrews, M. P.; Mattar, S. M.; Ozin, G. A. *J. Phys. Chem.* **1986**, *90*, 744.
(17) McCamley, A.; Perutz, R. N. *J. Phys. Chem.* **1991**, *95*, 2738.
(18) Lyon, J. T.; Andrews, L. *J. Phys. Chem. A* **2005**, *109*, 431.
(19) Debe, M. K. *J. Appl. Phys.* **1984**, *55*, 3354.
(20) Debe, M. K.; Kam, K. K. *Thin Solid Films* **1990**, *186*, 289.
(21) Parker, D. H.; Jones, M. E.; Koel, B. E. *Surf. Sci.* **1990**, *223*, 65.
(22) Hofmann, F.; Toennies, J. P. *Chem. Rev.* **1996**, *96*, 1307.
(23) Bain, C. D.; Troughton, E. B.; Tao, Y. T.; Evall, J.; Whitesides, G. M.; Nuzzo, R. G. *J. Am. Chem.* Soc. **1989**, *111*, 321.